EUROPEAN ORGANISATION FOR NUCLEAR RESEARCH

CERN/SPSLC 95-59/R106

EXPERIMENT PS209

Neutron halo and antiproton - nucleus potential from antiprotonic X rays

Report on June 1995 Run at LEAR

Run participants:

Warsaw University:	T. Czosnyka, K. Gulda, J. Iwanicki, M. Kisieliński, Z. Kondeja, P. Lubiński, P. Napiorkowski, L. Pieńkowski, A. Trzcińska
Technical University, München:	T. von Egidy, J. Hartmann
CERN:	J. Jastrzębski, W. Kurcewicz, E. Widmann
Institut des Sciences Nucleaires, Grenoble	D. Santos

Geneve, July 1995

Contents

A. RUN SUMMARY

The first run of the experiment PS209 was performed between June 6 and June 25, 1995. During the first week the antiproton beam momentum was, as long time ago scheduled, 300 MeV/c. Later this momentum was increased up to 400 MeV/c what made the PS209 running conditions much more difficult. Nevertheless, as a whole, the experiment was succesful. Basing on this we present below a request for the continuation during 1996.

At 300 MeV/c the following targets were investigated: ^{58}Ni, ^{64}Ni, ^{124}Te, ^{128}Te, ^{130}Te, ^{197}Au. At 400 MeV/c the investigated targets were: ^{59}Co, ^{58}Ni, ^{60}Ni, ^{62}Ni, ^{64}Ni, ^{172}Yb, ^{176}Yb, ^{197}Au, ^{208}Pb.

The objective of the PS209 experiment is the search for the manifestation of the extended neutron atmosphere in neutron rich nuclei via the study of the antiprotonic X rays. The observables of the experiment are:

(a) - the increase of the last observed level width due to the strong interaction effects;

(b) - the energy shift (in comparison with a pure electromagnetic energy) of the same level;

(c) - the increase of the before-last level width measured via the intensity balance of transitions populating and depopulating this level;

(d) - the absolute intensities of the antiprotonic X rays.

Observables (a) and (b) can only be extracted from the accumulated data after a long off-line spectra analysis. Therefore they will be not presented in this preliminary report.

A number of rough data related to the observable (c) were gathered during our run almost "on-line" and some of them are presented below.

Observable (d) was very difficult to obtain, especially due to the previously unexpected beam momentum increase and increased beam range straggling, larger than prepared target thicknesses. However, in some cases the absolute intensities will be deduced from the data using the radiochemical information collected for some targets. (The radiochemically determined mass yield distribution can be used as a measure of the antiproton flux absorbed by the target.)

The strategy selected to achieve the objectives of the experiment was to measure the light and heavy isotope of the same element and to search for isotopic differences in observables (a), (b) and (c). These differences, if not due to the E2 resonance or trivial changes in nuclear properties could be due to the extended nuclear atmosphere in heavy isotopes of a given element.

The most striking result of the present experiment could be the difference in the $n = 6 \rightarrow n = 5$ transition intensity observed between ^{58}Ni and ^{64}Ni (see Fig. 1, below). If confirmed, this result would signify almost two times larger upper level width in

^{64}Ni in comparison with ^{58}Ni. This effect could be due to the extended neutron atmosphere in the heaviest Ni isotope.

Care is, however, neccesary. Our data indicate that in the observed X-ray spectra a number of prompt, in beam gamma lines (in coincidence with $\overline{p}$) are present. Would such a gamma line be admixed in the 6 → 5 X-ray transition in ^{58}Ni and not present in ^{64}Ni - the observed isotopic effect could be much smaller or even disappear. The subsequent identification of the observed in-beam gamma lines, the consistency between the upper and lower level width changes in Ni isotopes and the next year cross-check measurements (see below) should help in reaching the final conclusions.

In even Te isotopes the increase of the upper level width between ^{124}Te and ^{128}Te is less pronouced, although clearly present. In ^{130}Te the E2 resonance mainly contributes to the much lower intensity of the n = 8 → n = 7 transition in this isotope in comparison with lighter Te isotopes.

In Yb isotopes the last observed transition is also weaker in heavier isotope although the effect is within presently assigned experimental errors.

The evaluation of the ^{208}Pb X-ray spectra may be useful for the precision of the $\overline{p}$ - nucleus potential in heavy nuclei.

The off-line gamma ray analysis of some targets is performed. This should allow us to determine the absolute X rays intensities in ^{128}Te, ^{176}Yb, ^{197}Au and ^{208}Pb isotopes. At the same time the neutron halo factor will be determined in ^{128}Te, the isotope previously not investigated by our radiochemical method of the nuclear surface study.

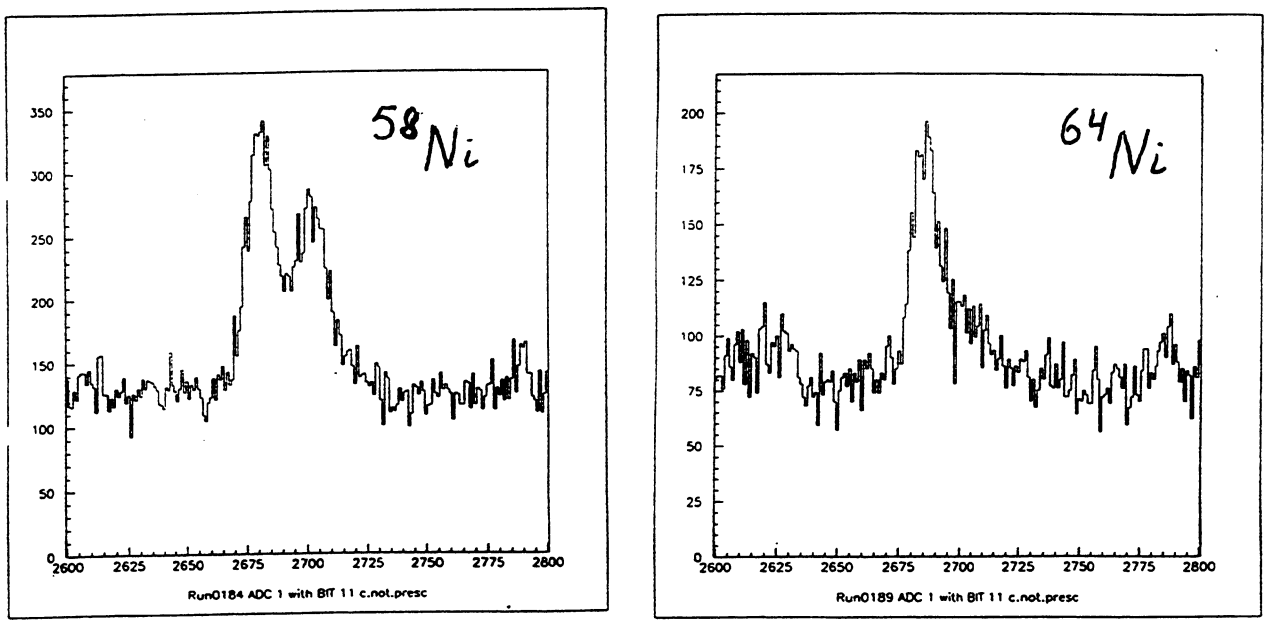

Fig. 1. The n = 8 → n = 6 (left hand side peak) and n = 6 → n = 5 (right hand side peak) antiprotonic X-ary transitions in ^{58}Ni and ^{64}Ni. Detector 1 spectra, taken at 300 MeV/c beam momentum.

In summary, whenever we were able to determine the differences in the last observed transition intensity between light and heavy isotope of the same element - always this intensity was smaller in the heavier one. This implies larger upper level width (stronger antiproton absorption) in heavier isotopes. This observation, although by itself not proving the existence of a neutron halo in heavier isotopes, is not in contradiction with such an assumption. The consistency between upper and lower level characteristics will be crucial in making final conclusions. Also, the confirmation of the observed here tendency for other elements will put these conclusions on a firmer ground.

B. BEAM TIME REQUEST FOR 1996

The preliminary data of this Report give the first evidence of the isotopic effects in the antiprotonic X-ray spectra for elements heavier than oxygen and not related to the E2 resonance. It is expected that, combined with our previous radiochemical studies, these data will be very helpful in the determination of the matter distribution in nuclear periphery. Therefore we propose to continue the investigation of the antiprotonic X rays within PS209 program during 1996. At present we foresee the following measurements:

(a) Targets close to ^{58}Ni in order to check the presence of the possible background lines of energy similar to the $6 \rightarrow 5$ transition in ^{58}Ni (^{56}Fe, ^{54}Fe).

(b) Search for isotopic effects in some of the following elements: Ca, Fe, Zn, Zr, Cd, Sn.

(c) Completion of the neutron halo study using radiochemical method. Neutron halo factor can be still determined in a few short lived nuclei using a simple rabbit system (no other special equipment necessary). In particular a very interesting case would be the ^{100}Mo target where a strong E2 effect makes the antiproton absorption probability more peripheral than in any other, previously investigated nucleus (a very large halo factor expected). Another exciting example would be the determination of the halo factor in double-closed shell nucleus, ^{48}Ca.

After consulting the LEAR coordinator, we ask for these measurements between 4 and 6 weeks (maximum available) of the 100 MeV/c antiproton beam, run in a parasitic modee with Obelix experiment. To our best knowledge there are no other request for parasiting this experiment in 1996.

C. EXPERIMENTAL DETAILS OF 1995 RUN

1. Beam line

The M1 beam line was allocated for this experiment. Fig. 2 shows the last part of this line together with the placement of two HPGe detectors.

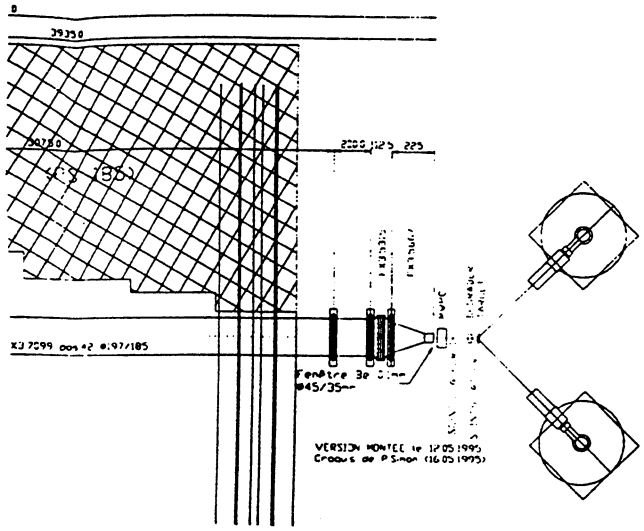

Fig. 2. End part of the M1 beam line.

2. Germanium Detectors

The dimensions of two HPGe detectors used on-line were:

Det. 1 490 $mm^2 \times 13$ mm

Det. 2 1893 $mm^2 \times 49.5$ mm

A third detector of about 30 % efficiency was used for the off-line gamma ray spectra measurements. Their energy resolution is shown in Fig. 4 at the beginning of their in-beam operation.

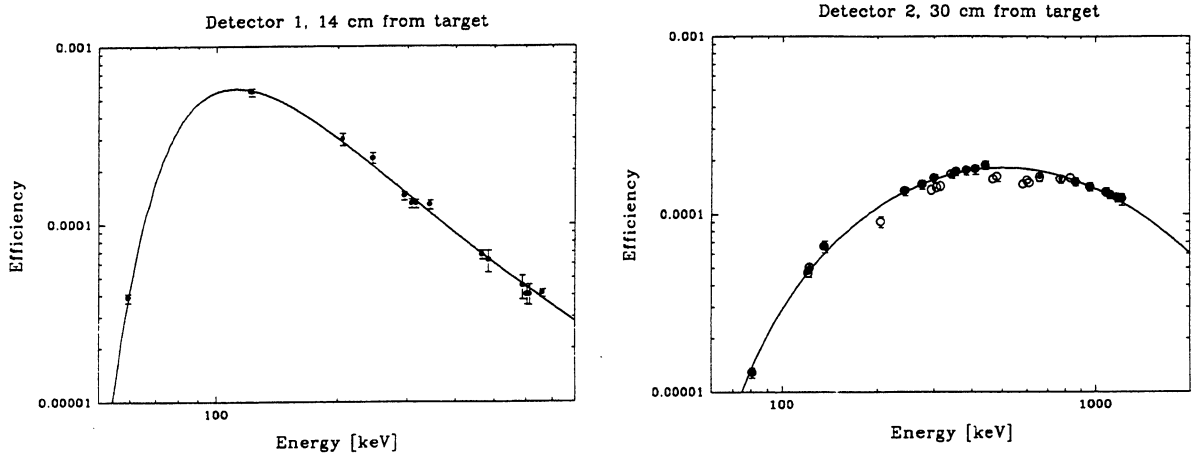

Fig. 3. Absolute gamma-ray efficiency for two detectors used in beam in PS209 June run.

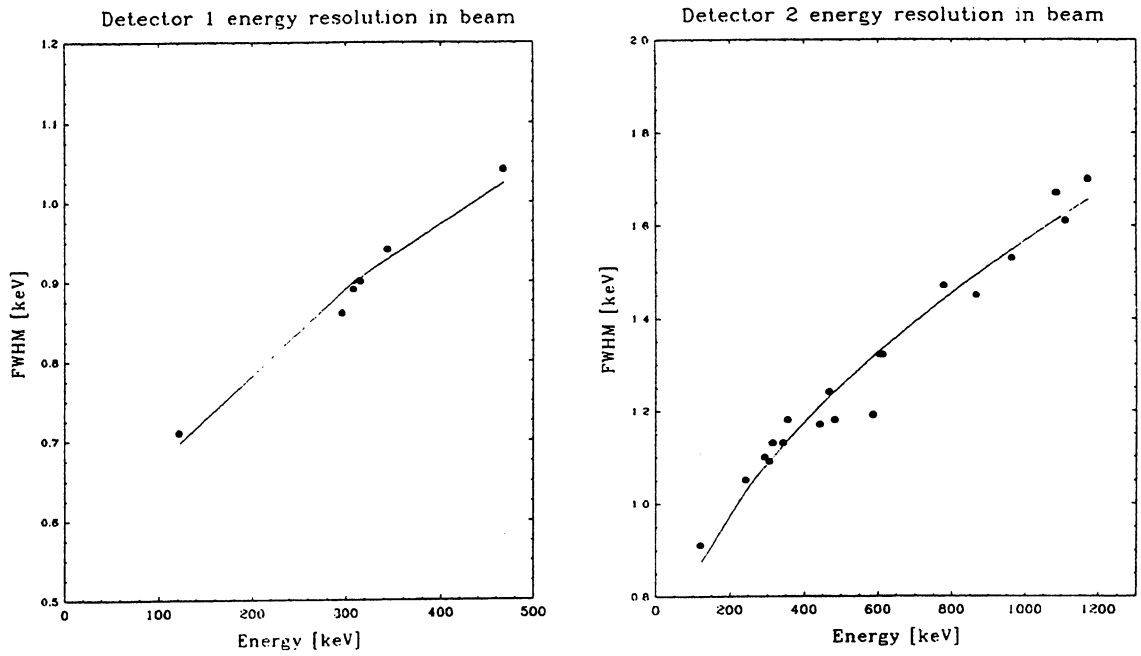

Fig. 4. Energy resolution of two detectors working in-beam at the beginning of the run.

3. Antiproton beam

The beam momentum during the first week of operation was 300 MeV/c with an excellent spill shape (see Fig. 5). When the beam momentum was increased to 400 MeV/c the main user, Obelix, requested a very high antiproton intensity what resulted in a very unfavourable spill shape for PS209 (see Fig. 6). Eventually, after some difficult days much more favourable spill shape was obtained (see Fig. 8).

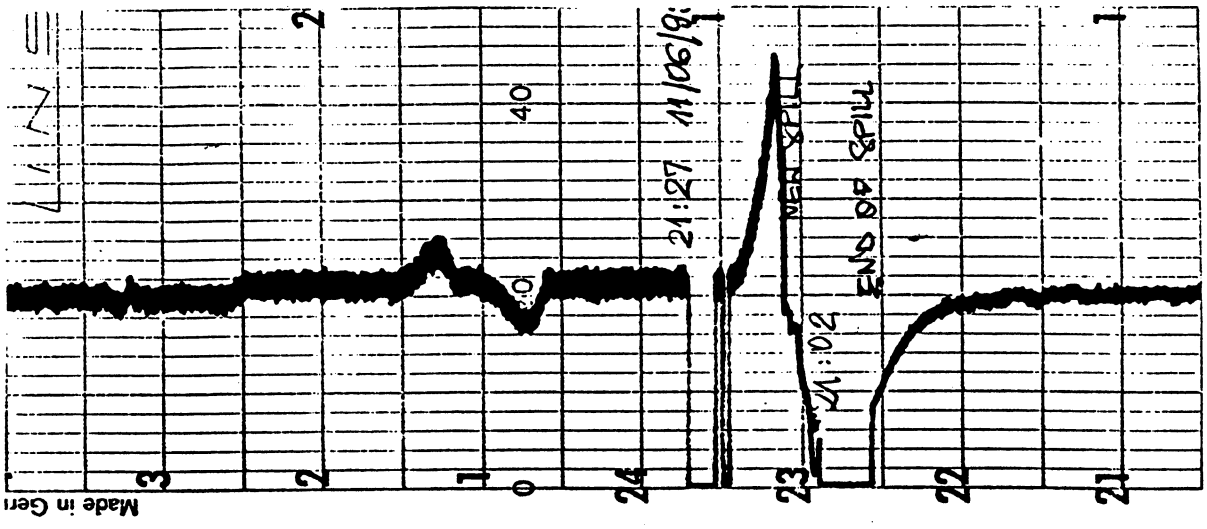

Fig. 5. Example of a spill shape at 300 MeV/c. Obelix and PS209 take about the same number of antiprotons (50 $k\bar{p}$/s). Long spills, up to 14 h duration, were achieved (11.06.95). Writer speed: 5 cm/h.

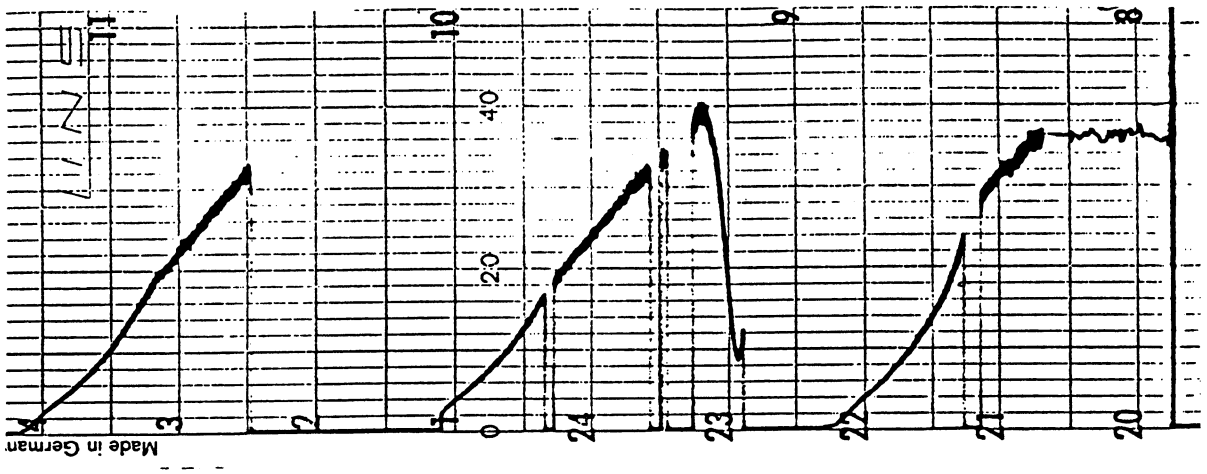

Fig. 6. Spill shape examples at the beginning of 400 MeV/c beam. Obelix takes about 2.5×10^6 $\bar{p}$ps, PS209 about 50×10^3 $\bar{p}$ps (15.06.95).

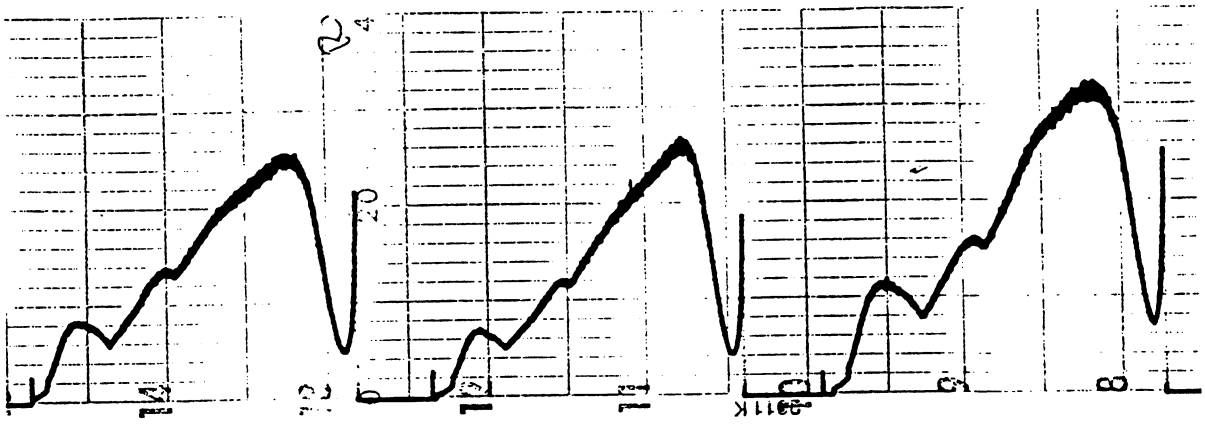

Fig. 7. First attempts to change the cooling during the spill in order to achieve a more flat spill shape for PS209 (20.06.95).

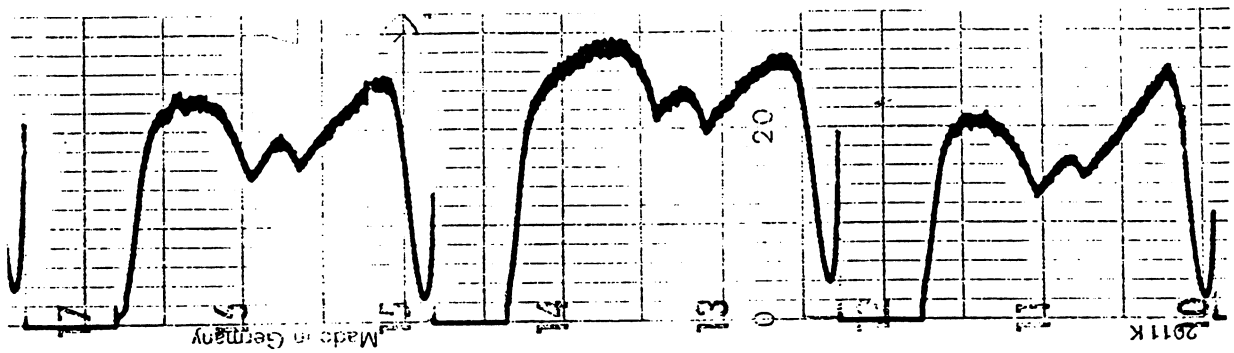

Fig. 8. Succesful change of the beam cooling during the spill, PS209 obtains much more uniform antiproton intensity (22.06.95).

4. Electronics

The scheme of electronics used is shown in Fig. 9. Signals from the antiproton detectors S1, S2 were discriminated against noise by 2 fast discriminators with a threshold set about 0.8 MeV and next sent to the AND gate circuit for 10 ns overlap indicating the passage of antiproton. Pulses from one (300 MeV/c run) or two (400 MeV/c run) HPGe detectors were sent into energy spectrometric and fast timing branches. The energy spectrometric one involved ORTEC 672 spectroscopy amplifier with 6 μs shaping time and unipolar output for the best energy resolution. Signal from the amplifier was digitised by 8k ORTEC AD413A CAMAC ADC. Fast timing branch was splitted immediately into two paths both involving timing filter amplifier (differentiation = 200 ns, integration out) followed by constant fraction discriminator. The combination of gains and thresholds was to let high energy pulses from pions and charged particles only pass in one path (high threshold) while from gammas also in another one (low threshold).Since pions and charged particles deposit tens of MeVs in the detector the preamplifier was saturated and not operative for some 500 μs. Thus 600 μs wide , retriggerable gate generator followed high threshold discriminator.Its output was used to reject delayed by 32 ns low threshold discriminator signal. Thus pions rejection was accomplished and only gamma signals were let through.

Various AND, OR, Rate Divider NIM modules helped to make trigger. The trigger was generated if

1. the coincidence with antiproton took place;
2. every n^{th} gamma signal was detected (scaling down) to allow calibration source lines recording on-line;
3. pulser (10 ppm/^{o}C stable 0.5 pps rate) was present at the time in anticoincidence with pion for stability monitoring;

   and finally

4. every each second to read contents of various scalers.

A time spectrum gamma - antiproton was taken with LeCROY TDC 4208 in CAMAC. The FWHM of prompt peak was about 11 ns for 60-800 keV energy range of gammas and no attempt was made to optimise time resolution.

Several Gate&Delay modules helped to accommodate the above described electronics to the data acquisition system STARBURST (bit pattern, ADC gates, busy logic).

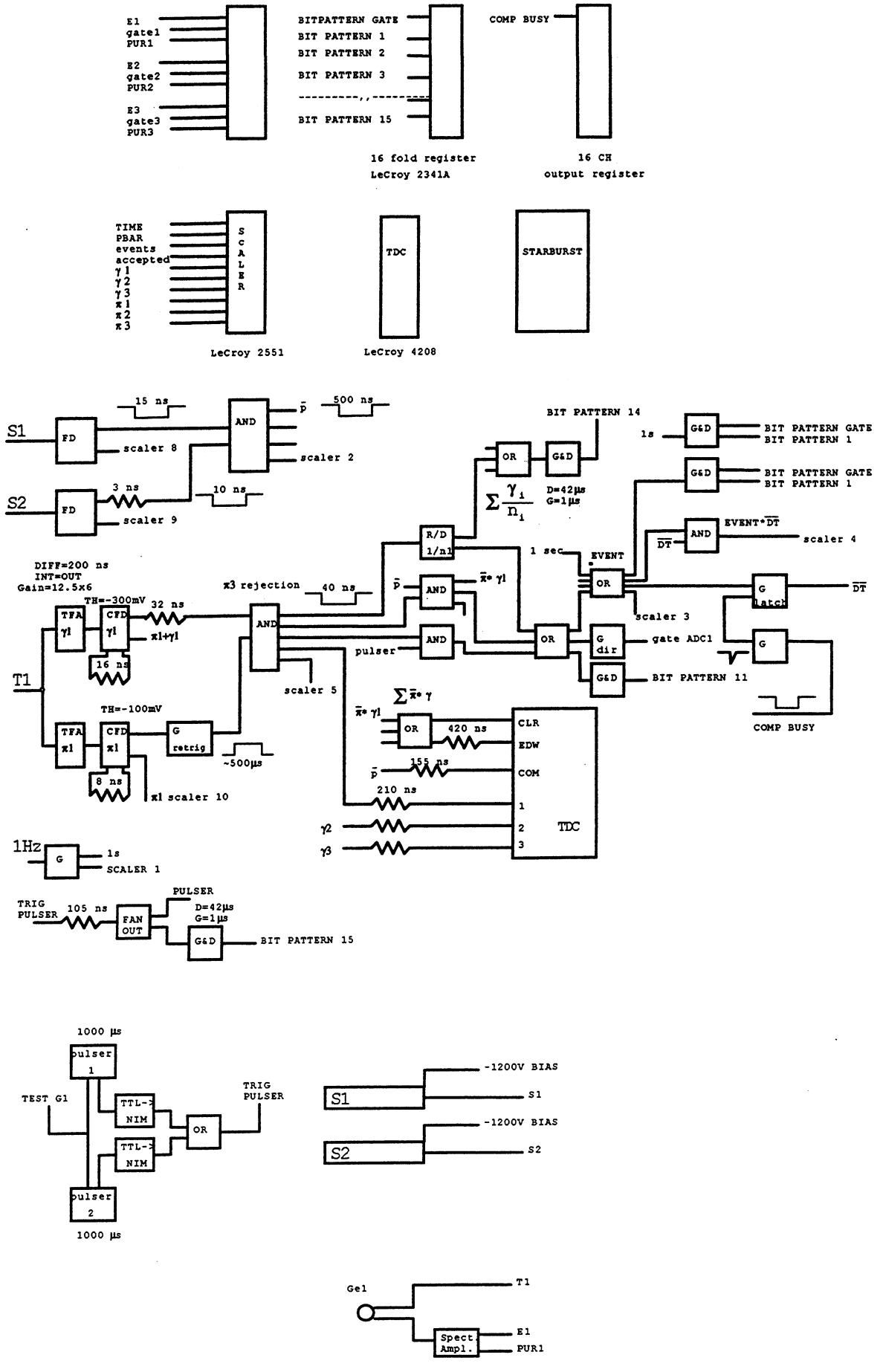

Fig. 9. Scheme of electronics used for PS-209 experiment in June 1995.

The rates in optimal counting conditions were , approximately:

antiprotons in S1	40×10^3 cps,
antiprotons in S2	32×10^3 cps,
pions in Ge1	200 cps,
gammas in Ge1	600 cps,
coincidences Ge1-antiproton	80 cps,
pions in Ge2	600 cps,
gammas in Ge2	500 cps,
coincidences Ge2-antiproton	100 cps.

5. Data Acquisition System

Data acquisition system for PS209 experiment was based on the CES STARBURST J11 module working in CAMAC crate. It worked with BIT PATTERN unit (LeCroy 2341A) to recognise the type of event and CAMAC-SCSI interface (KINETIC SYSTEMS K3929) to connect crate to acquisition computer (VAX station 4000 VLC).

Mainly two programs were running on the acquisition computer:

- EXP - to program and control STARBURST module, to on-line analyse the events, to write events on disk,
- PAW - to display results of on-line sort.

Scheme of acquisition system is shown in Fig. 10.

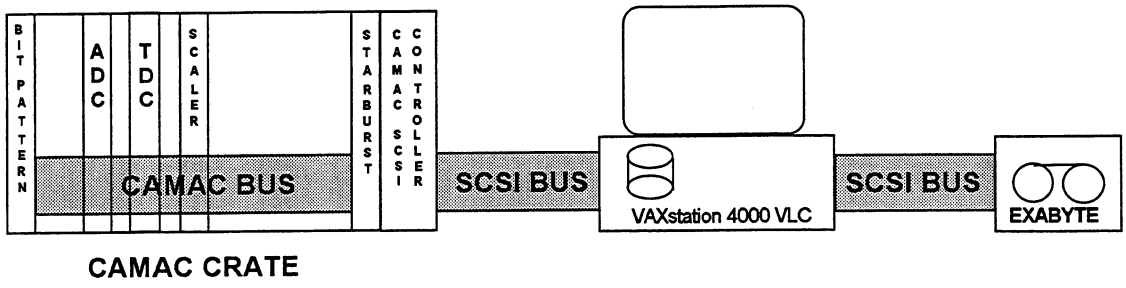

Fig. 10. Scheme of acquisition system

Main features of the data collection

Program running on STARBURST was looking at states of BIT PATTERN unit placed in CAMAC slot nr 1. If any of its inputs was active, the system started the procedure of readout of modules in crate according to the number of active input. Data were formed into events and collected in buffer memory of STARBURST. Full buffer

was sent to acquisition computer by CAMAC-SCSI controller, analysed by on-line sorting program and written on disk. Event files were stored on EXABYTE tape later.

Four parameters: times and energy of X rays in two germanium detectors were measured. Additionally 10 parameters were counted with scaler and written into event file to monitor the data acquisition.

Maximum counting rate of the acquisition system was about 300 events per second. During the experiment typical dead time of was 5 %, but never larger than 20 %.

Structure of the event

Structure of event is as follows:

- header (4 words - 32 bytes) contains length, type, number of the event and a control word (always equal 19785),
- data of event.

There were two types of events:

- scaler's event generated typically every 10 seconds,
- gamma's event generated by experimental conditions.

Scaler's event contains only readout of LeCroy 2551 scalers module, which indicates:

- seconds of the run,
- S1, S2 counters' coincidences,
- events,
- accepted events,
- gamma-rays in germanium detectors (3 channels of scaler),
- antiprotons in plastic scintillators(2 channels),
- pions in germanium detectors (3 channels).

Length of scaler's event with header is 28 words (56 bytes).

Gamma's event contains 3 words of ADC(ORTEC AD413A) and 6 words of TDC (LeCroy 4208) module readout. Except of it type of event word in event header contains information about experimental conditions of master trigger generation (antiproton coincidence, prescaled single gamma-ray, pulser). Meanings of bits in type of event word are shown in table below.

Length of gamma's event with header is 13 words (26 bytes).

Table. I. Meanings of high state of bits in type of event word of event header.

Bit	Interpretation
0	scaler's event
1	gamma's event
2-10	not used
11	gamma in det. 1 and antiproton coincidence
12	gamma in det. 2 and antiproton coincidence
13	not used
14	prescaled single gamma
15	pulser event

On-line analysis

Incoming events were sorted by user subroutine of EXP program into one and two dimensional histograms and displayed with PAW.

X-ray cascade from antiprotonic atom was observed as one dimensional energy spectra which were created with different conditions and gates (e.g. on time prompt peak).

Many tools were used to monitor data acquisition additionally. Statistics of runs were shown on printout of scaler (see description of scaler event). Counting rates in different parts of detection system were displayed as function of time. On "S1S2" plot were shown:

- counting rate in S1 and S2 plastic scintillators to monitor shape of the spill,
- ratio of S1/S2 counts to monitor the focusing of the beam,
- counting rate of collected events (ACCEPTED VS TIME),
- ratio of generated triggers to accepted by ACQ system to monitor the dead time of acquisition,
- counting rate of X-rays and pions in both germanium detectors.

Two-dimensional plot of pulser counts vs time was used to monitor the stability of electronics. Mean value of pulser peak in energy spectrum and pulser's counts per 200 s were also displayed as function of time of run.

D. SOME EXPERIMENTAL RESULTS

1. Ni isotopes

After the observation of a large isotopic effect between ^{58}Ni and ^{64}Ni (see Sec. A) at 300 MeV/c, targets of ^{60}Ni and ^{62}Ni were prepared and measured at 400 MeV/c beam. Fig. 11. shows the lines of interest in four investigated Ni isotopes. In Fig. 12. the yield of the 6 → 5 transition as a function of the target mass is shown.

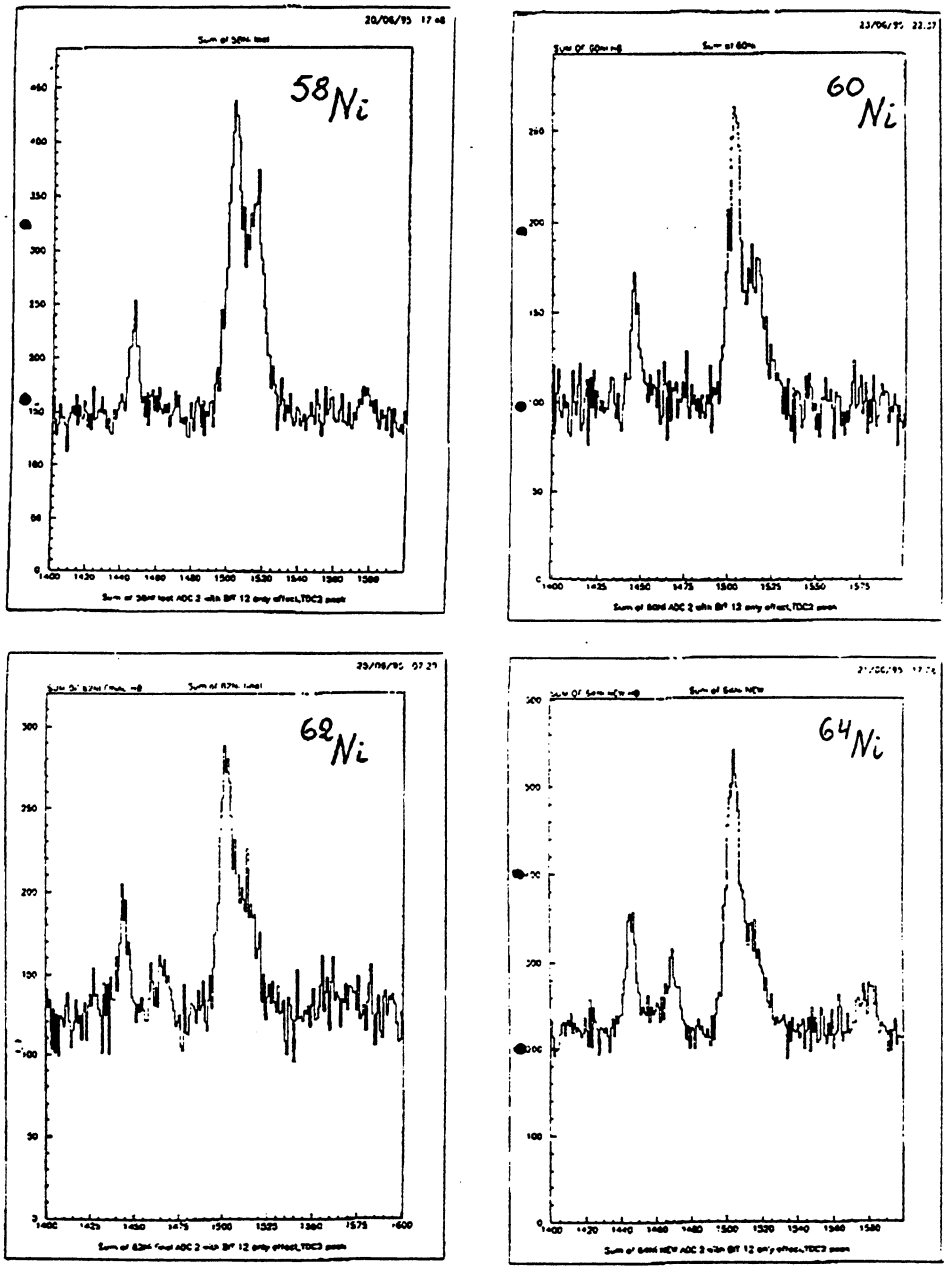

Fig. 11. The n = 8 → n = 6 and n = 6 → n = 5 doublet in even Ni isotopes. Detector 2 spectra taken at 400 MeV/c beam momentum. Compare also Fig. 1.

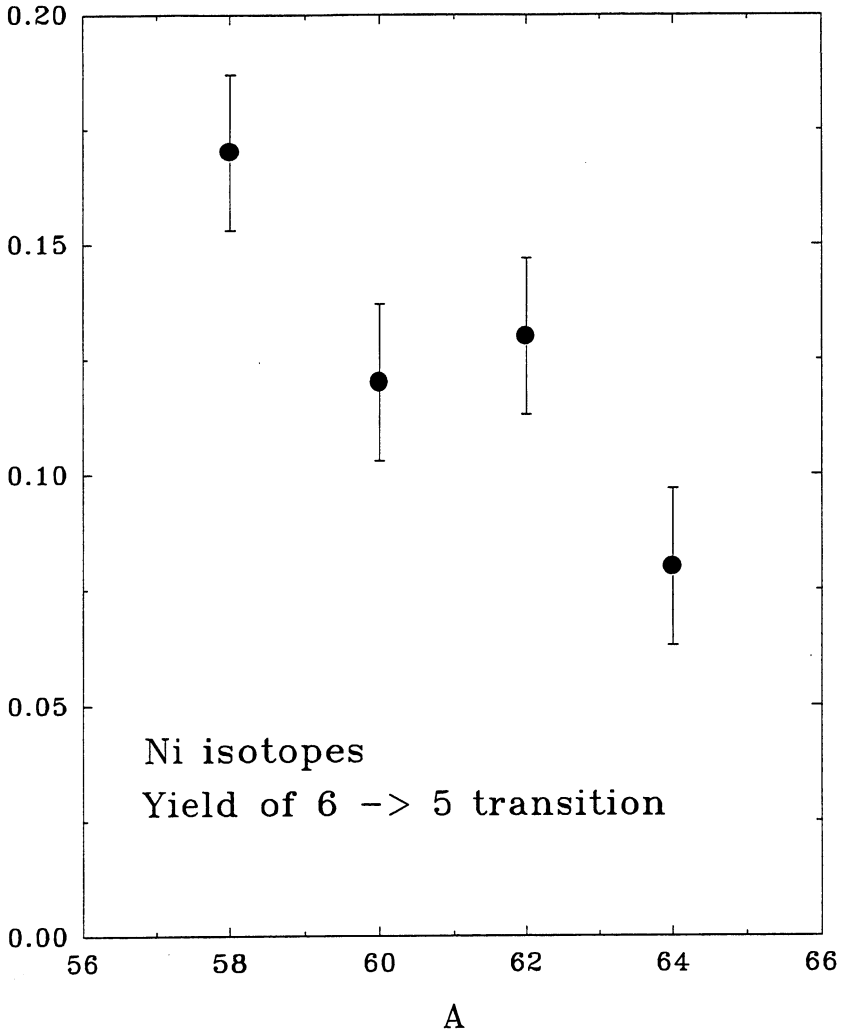

Fig. 12. The relative yield of the 6 → 5 transition (obtained from the X-ray intensity balance of n = 6 level, Auger transitions neglected) as a function of Ni isotope mass number, A. The yield from 400 MeV/c data is presented.

2. Te isotopes

Fig. 13. shows the L-S doublet of the n = 8 → n = 7 transition and Fig. 14. the yield of this transition as a function of Te mass number A.

In ^{130}Te a strong E2 resonance effect makes this yield very small. It is not clear at present how this effect contributes to the systematics decrease with A of the 8 → 7 transition intensity in lighter Te isotopes.

It is interesting to note that the intensity ratio of the L-S lower - higher energy doublet is visibly larger in ^{130}Te in comparison with lighter isotopes. This ratio is 1.27, 1.33 and 1.59 for ^{124}Te, ^{128}Te and ^{130}Te, respectively. This can be probably easily understood. The energy difference between Δn = 2 resonating levels (n = 8 and n = 6) and the 2^+ level is in ^{130}Te negative (the average value equal to - 21.8 keV), so the higher energy component having this value "less negative" should "resonate better". This is, indeed, observed.

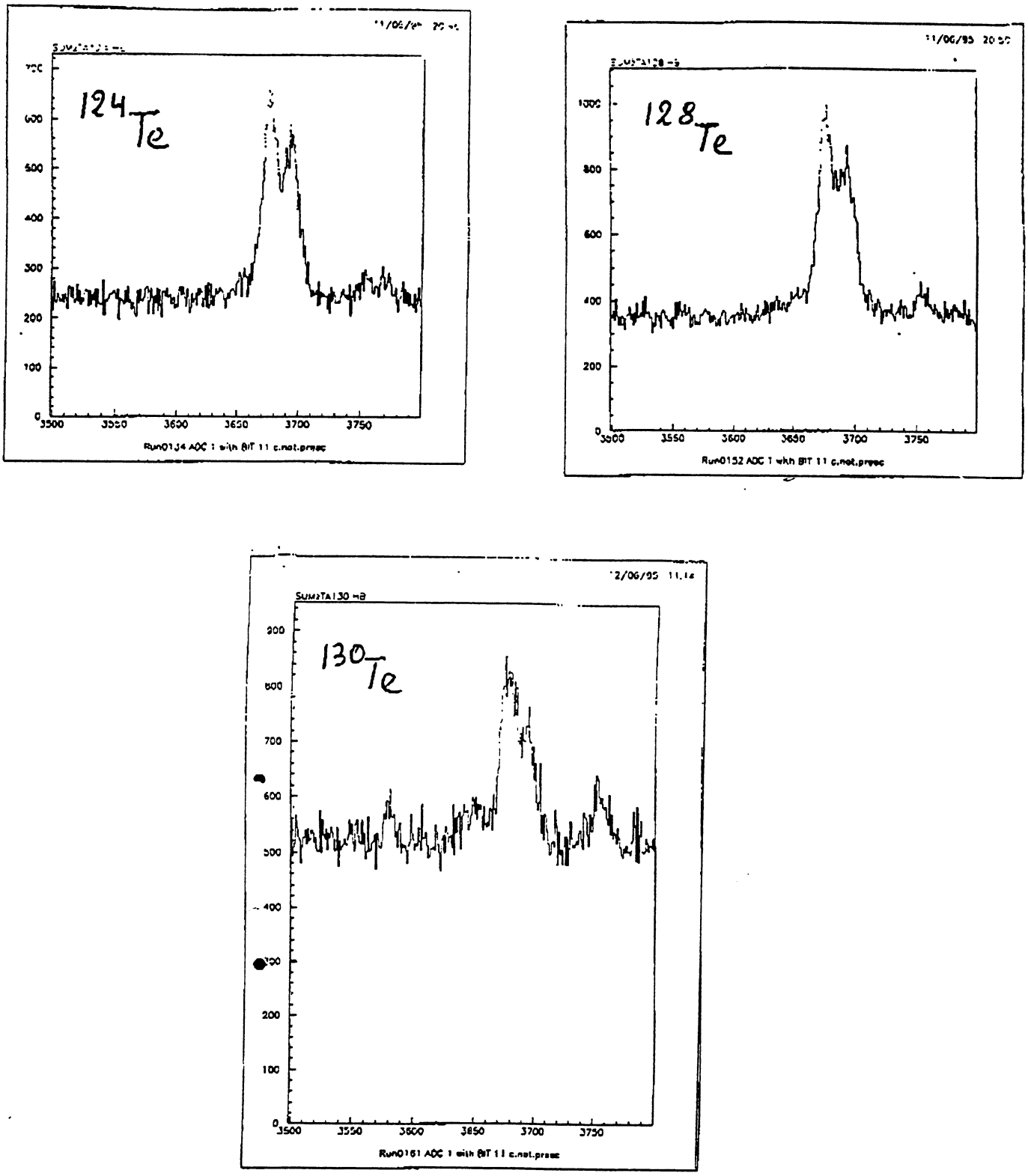

Fig. 13. The L-S doublet of the $n = 8 \rightarrow n = 7$ transition in even Te isotopes. Detector 1 spetra taken at 300 MeV/c beam momentum.

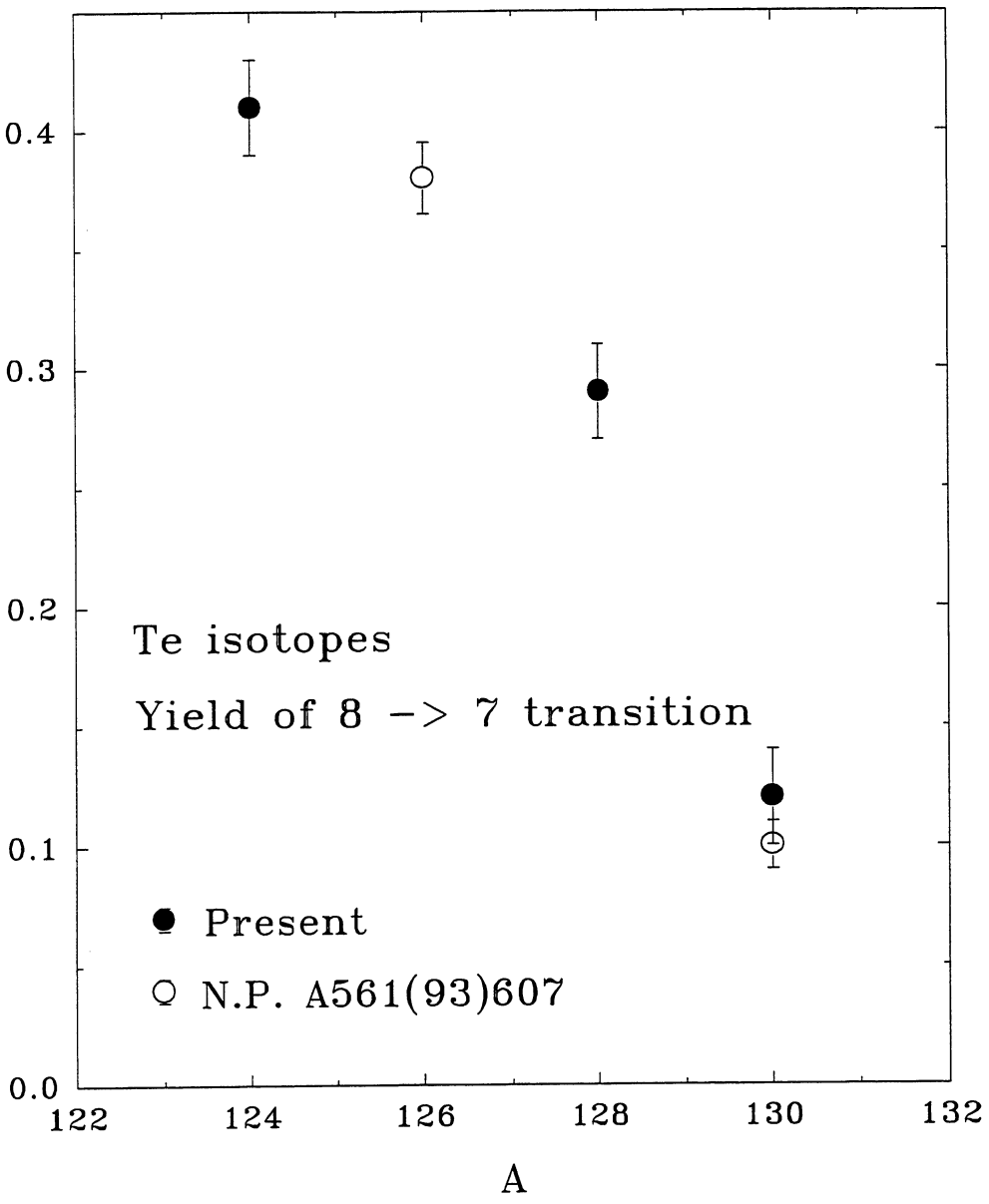

Fig. 14. The relative yield of the 8 → 7 transition as a function of Te isotopes mass number, A.

3. Yb isotopes

The ^{172}Yb and ^{176}Yb were measured at 400 MeV/c beam momentum. The n = 9 → n = 8 L-S doublet for ^{176}Yb is shown in Fig. 15. for two detectors used. Data of similar quality were obtained for ^{172}Yb. The relative yield of the 9 → 8 transition in both isotopes is shown in Fig. 16.

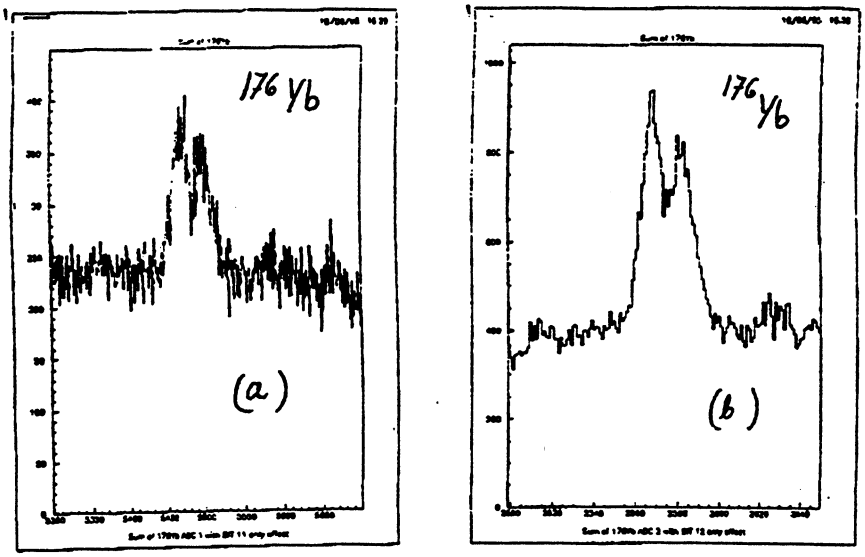

Fig. 15. The L-S doublet of the $n = 9 \rightarrow n = 8$ transition in ^{176}Yb measured at 400 MeV/c beam momentum. The preliminary peak energies are 402.3 keV and 404.7 keV. (a) Detector 1. (b) Detector 2.

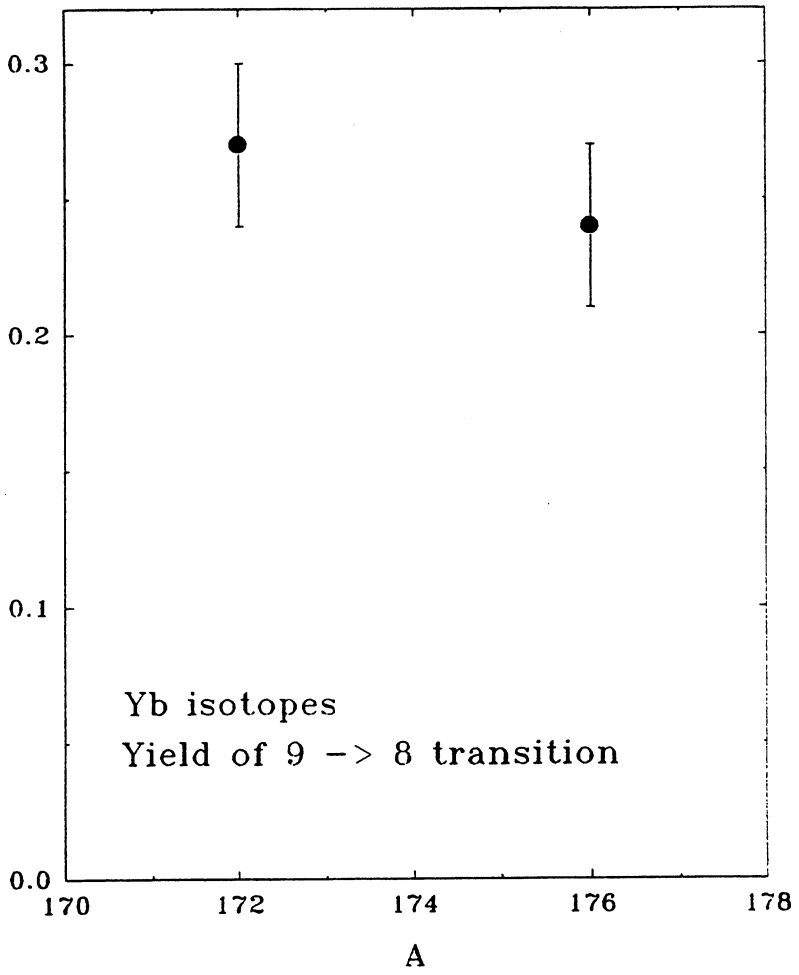

Fig. 16. The relative yield of the $9 \rightarrow 8$ transition as a function of Yb isotopes mass number, A.